

# Measurements of spin reorientation in $\text{YbFeO}_3$ and comparison with modified mean-field theory

Ya. B. Bazaliy,<sup>1,2</sup> L. T. Tsymbal,<sup>2,3</sup> G. N. Kakazei,<sup>3,4</sup> V. I. Kamenev,<sup>2</sup> and P. E. Wigen<sup>3</sup>

<sup>1</sup>IBM Almaden Research Center, 650 Harry Road, San Jose, California 95120, USA

<sup>2</sup>O.Galkin Donetsk Physics & Technology Institute, National Academy of Science of Ukraine, R. Luxemburg Street 72, Donetsk, 83114 Ukraine

<sup>3</sup>Ohio State University, Department of Physics, 174 West 18th Avenue, Columbus, Ohio 43210, USA

<sup>4</sup>Institute of Magnetism, National Academy of Science of Ukraine, 36-B Vernadskii Boulevard, Kyiv, 03142 Ukraine

(Received 2 March 2005; revised manuscript received 26 July 2005; published 1 November 2005)

Precise measurements of  $\text{YbFeO}_3$  magnetization in the spin-reorientation temperature interval are performed. It is shown that ytterbium orthoferrite is well described by the modified mean-field theory recently developed for  $\text{ErFeO}_3$ . This validates the conjecture about the essential influence of the rare-earth ion's anisotropic paramagnetism on the magnetization behavior in the reorientation regions of all orthoferrites with  $\Gamma_4 \rightarrow \Gamma_{24} \rightarrow \Gamma_2$  phase transitions.

DOI: [10.1103/PhysRevB.72.174403](https://doi.org/10.1103/PhysRevB.72.174403)

PACS number(s): 75.30.Kz, 75.10.Hk, 75.50.Dd, 75.50.Ee

## I. INTRODUCTION

Rhombic rare-earth orthoferrites  $R\text{FeO}_3$  with  $R$  being a rare-earth ion or an yttrium ion are magnetic insulators that provide a classic example of the second order orientation phase transitions (see reviews<sup>1-4</sup>). Orthoferrites have two magnetic subsystems: one of the rare-earth ions, and another of the iron ions. Magnetic properties of the subsystems and interaction between them depend on the external parameters, e.g., temperature, field, pressure, etc., and a series of phase transition is observed upon the parameter change. The field of spin-reorientation transitions in orthoferrites experiences a surge of interest after the observations of picosecond spin rotation times in those materials<sup>5,6</sup> with ramifications for the future device applications.

Orientation phase transitions discussed in this paper are characterized by the following.<sup>1</sup> The iron subsystem is ordered into a slightly canted antiferromagnetic structure exhibiting a weak ferromagnetic moment  $\mathbf{F}$ . The rare-earth system is paramagnetic. For all orthoferrites the antiferromagnetic structure below the Neel temperature  $T_N$  ( $T_N = 620-740$  K) corresponds to the  $\Gamma_4$  ( $G_x, F_z$ ) irreducible representation with magnetic vector  $\mathbf{F}$  pointing along the  $\mathbf{c}$  axis of the crystal and antiferromagnetic vector  $\mathbf{G}$  pointing along the  $\mathbf{a}$  axis (coordinates are chosen so that  $\mathbf{c} = \hat{z}$  and  $\mathbf{a} = \hat{x}$ ). In orthoferrites with nonmagnetic rare-earth ions ( $R = \text{La, Lu, or Y}$ ) the  $\Gamma_4$  ( $G_x, F_z$ ) configuration persists to the lowest temperatures. For many other orthoferrites, such as  $\text{ErFeO}_3$ ,  $\text{TmFeO}_3$ ,  $\text{YbFeO}_3$ ,  $\text{NdFeO}_3$ ,  $\text{SmFeO}_3$ , a reorientation transition with the sequence  $\Gamma_4$  ( $G_x, F_z$ )  $\rightarrow$   $\Gamma_{24}$  ( $G_x, F_x$ )  $\rightarrow$   $\Gamma_2$  ( $G_z, F_x$ ) is observed. Upon cooling vector  $\mathbf{F}$  starts to rotate away from the  $\mathbf{c}$  axis at temperature  $T_1$ . Its continuous rotation towards the  $\mathbf{a}$  axis happens in the  $(\mathbf{a}, \mathbf{c})$  plane between temperatures  $T_1$  and  $T_2 < T_1$ . Below  $T_2$ , the system stays in the  $\Gamma_2$  ( $G_z, F_x$ ) phase with  $F \parallel \mathbf{a}$ .

Although the spin reorientation region  $[T_2, T_1]$  has been studied for many orthoferrites by different experimental techniques,<sup>1-3</sup> not enough is known about the specifics of the rotation. Relevant experimental results are often incomplete, lack accuracy, tend to contradict each other, and do not cor-

respond to either conventional Landau theory<sup>2,7,8</sup> or its suggested modifications. Recently<sup>9,10</sup> the temperature dependence of both  $\mathbf{a}$  and  $\mathbf{c}$  axis projections of the magnetic moment was measured with high accuracy for the single crystal samples of  $\text{ErFeO}_3$ . These measurements gave the temperature dependence of the absolute value of the magnetization  $M(T)$  and its rotation angle  $\theta(T)$  with respect to the  $\mathbf{c}$  axis in the  $[T_2, T_1]$  temperature interval at zero external magnetic field. The results were in very good agreement with the proposed modified mean-field model,<sup>9</sup> that emphasized the anisotropy of the rare-earth ions paramagnetic susceptibility. It was conjectured that this model would be suitable for other magnetic materials with similar phase transitions.

The present study is aimed at the detailed measurements of  $M(T)$  and  $\theta(T)$  behavior in single crystals of  $\text{YbFeO}_3$ , that exhibit the same  $\Gamma_4 \rightarrow \Gamma_{24} \rightarrow \Gamma_2$  transition, with the purpose of checking this conjecture on another material. It is shown that the modified field theory of Refs. 9,10 works well for  $\text{YbFeO}_3$ , even though in this orthoferrite the reorientation happens at an order of magnitude lower temperatures ( $T \approx 8$  K), than in  $\text{ErFeO}_3$  ( $T \approx 90$  K), while the Neel temperature remains roughly the same  $T_N \approx 630$  K.

## II. EXPERIMENTAL RESULTS

Measurements were performed on two single crystals of  $\text{YbFeO}_3$ . Cubic sample A, weighting 0.0485 g, was made of a single crystal grown by spontaneous crystallization in the melt solution. Sample B had ellipsoidal shape, weighted 0.0715 g, and was made of a single crystal grown by the no-crucible zone melting technique with radiation heating. The temperature was varied in the 2 to 10 K interval, and both  $M_a$  and  $M_c$  projections of the magnetic moment were sequentially measured on samples A and B by a Quantum Design MPMS-5S SQUID magnetometer as described below. The magnetization values obtained on two samples were very similar. This is consistent with the fact that the magnetization of the orthoferrite is weak and the demagnetization fields are too small to create an appreciable shape dependence of the results.

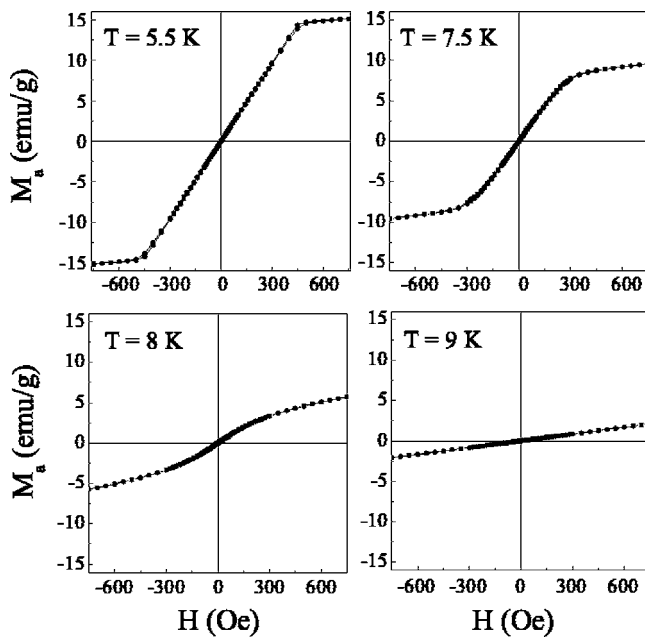


FIG. 1. Magnetization curves  $M_a(H)$  obtained on YbFeO<sub>3</sub>, sample B, with  $H\parallel a$ , at different temperatures.

The  $M(T)$  dependence at zero external magnetic field was found through the analysis of magnetization loops. In YbFeO<sub>3</sub> they are S shaped at all temperatures studied here for both  $H\parallel a$  and  $H\parallel c$  field orientations (Figs. 1 and 2). Importantly, magnetization curves obtained for different samples are very similar. The  $M_a$  and  $M_c$  projections of the bulk magnetization at zero external field were extracted from the hysteresis loops measured in magnetic fields directed along the  $a$  and  $c$  axes, respectively. The linear  $M(H)$  dependence observed at higher fields  $H \geq 650$  Oe was fitted by a line  $M_{a,c}(H, T) = M_{a,c}(T) + \chi_{a,c}(T)H$  and the vertical intercept  $M_{a,c}(T)$  was recorded. The values of  $M_a(T)$  and  $M_c(T)$  ob-

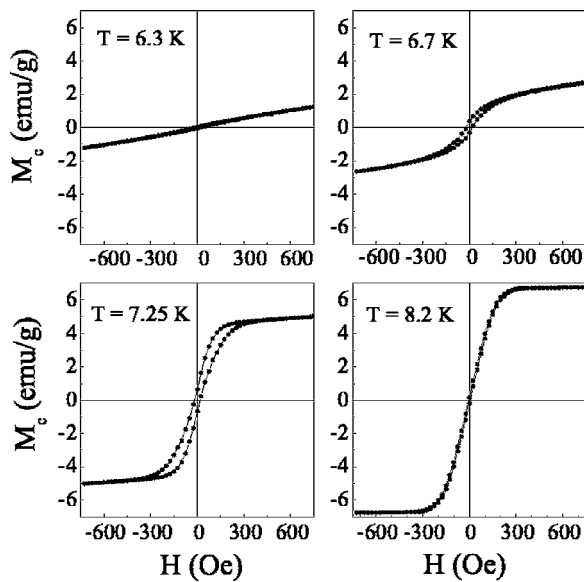


FIG. 2. Magnetization curves  $M_c(H)$  obtained on YbFeO<sub>3</sub>, sample A, with  $H\parallel c$ , at different temperatures.

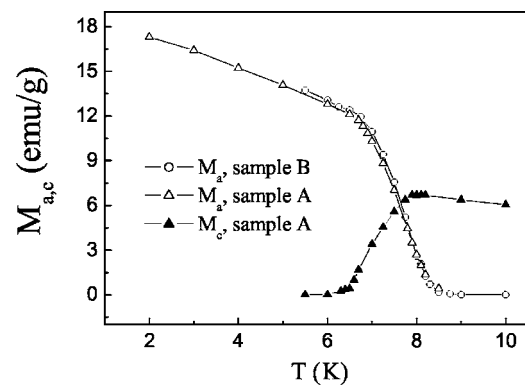


FIG. 3. Magnetization projections  $M_{a,c}(T)$  obtained from the magnetization curves. Empty circles:  $M_a(T)$  for sample B, empty triangles:  $M_a(T)$  for sample A, filled triangles:  $M_c(T)$  for sample A.

tained through this procedure are shown in Fig. 3.

To analyze the data we recall, that the  $(H-T)$  phase diagrams in the vicinity of the  $\Gamma_4 \rightarrow \Gamma_{24} \rightarrow \Gamma_2$  transition for  $H\parallel c$  and  $H\parallel a$  field directions are well known.<sup>2</sup> According to these diagrams, as the magnetic field is swept through  $H=0$  inside the  $[T_2, T_1]$  reorientation interval, a first order transition happens for both directions of the field and manifests itself as a jump of magnetization component parallel to the applied field. First-order transitions also happen above  $T_1$  for  $H\parallel c$  and below  $T_2$  for  $H\parallel a$  orientations, while no transitions are predicted below  $T_2$  for  $H\parallel c$  and above  $T_1$  for  $H\parallel a$ . Indeed it is observed that magnetization curves become straight lines passing through the origin above  $T_1$  for the  $H\parallel a$  orientation and below  $T_2$  for the  $H\parallel c$  orientation (see Figs. 1 and 2). In a real experiments exact orientation of the field direction is obviously impossible. A three-dimensional diagram valid for the arbitrary field direction<sup>9,11</sup> should be used in this case.

The shapes and sizes of hysteresis loops reflect the mode of magnetic reversal and the physics of magnetic domains and domain walls in a material. These matters are beyond the scope of the present paper. Here we simply note that the evolution of hysteresis loops with temperature in ytterbium orthoferrites differs substantially from the one observed in erbium orthoferrite.<sup>9</sup> No rectangular loops were observed in YbFeO<sub>3</sub>, while in ErFeO<sub>3</sub> they are seen outside of the reorientation region. But, similar to the case of ErFeO<sub>3</sub>, it was found that the parameters of the loop, e.g., remanent magnetization, exhibit singular behavior near the transition points  $T_1$  and  $T_2$  (Fig. 4). In this experiment a saturating magnetic field  $H=650$  Oe was applied either along the  $a$  or along the  $c$  axis. Then, the field was reduced to zero and the projection of the remanent magnetic moment  $M^{\text{remanent}}$  on the same axis was measured. Two series of measurements, one for  $M_c^{\text{remanent}}$  and another for  $M_a^{\text{remanent}}$  were made. The results for the  $H\parallel c$  case are shown on Fig. 4, where two kinks near  $T_1$  and  $T_2$  are clearly seen. Similar results were obtained for  $H\parallel a$ . This property of the hysteresis loops turns out to be useful for the determinations of the critical temperatures  $T_{1,2}$ . For the example the curve on Fig. 4 gives  $T_1=8$  K and  $T_2=6.6$  K.

The absolute value of magnetization  $M$  and rotation angle  $\theta$  were extracted from the experimental data according to the expressions

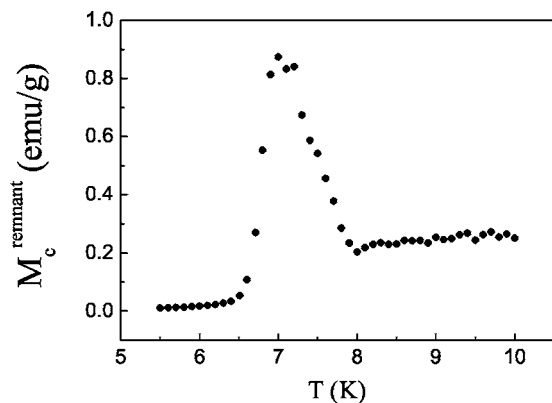


FIG. 4. Temperature dependence of remanent magnetization along the  $c$  axis. The kinks of the curve mark the transition temperatures  $T_{1,2}$ .

$$M = \sqrt{M_a^2 + M_c^2}, \quad \theta = \arctan\left(\frac{M_a}{M_c}\right)$$

and are shown in Figs. 5 and 6. Experimental results presented in Figs. 3 and 5 show that as the temperature is lowered from  $T_N$  to  $T_1$ , the magnetization of the crystal gradually grows. This reflects the build up of the iron moment near  $T_N$  and subsequent development of the ytterbium moment along iron moment<sup>1</sup> at lower temperatures. In the narrow reorientation region  $[T_2, T_1]$  the magnetization rapidly grows almost twofold. Below  $T_2$  the magnetization continues to grow. This supports the result of Ref. 12, suggesting that the ytterbium moment remains parallel to the iron moment, and does not switch to the antiparallel direction as stated in Ref. 1.

### III. THEORETICAL ANALYSIS

Our experimental results can be explained by the modified mean field theory proposed in Refs. 9,10. As the conventional Landau theory,<sup>2,7,8</sup> the modified theory assumes that the magnetization of iron subsystem is saturated at  $T \lesssim T_{1,2}$

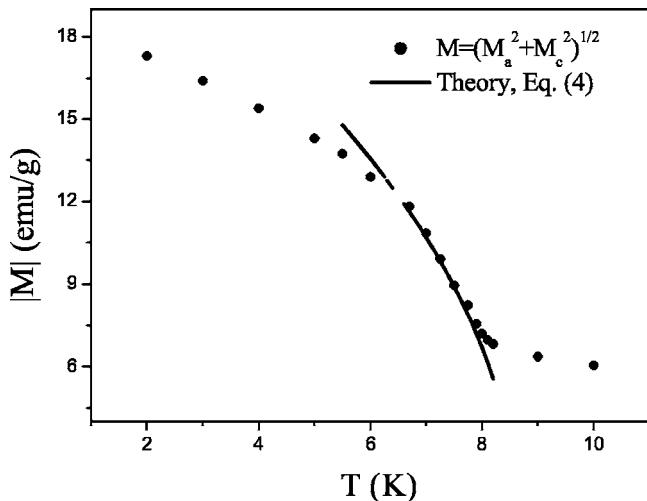


FIG. 5. Absolute value of the magnetization  $M(T)$  calculated from experimental data. Solid curve: theory Eq. (4)

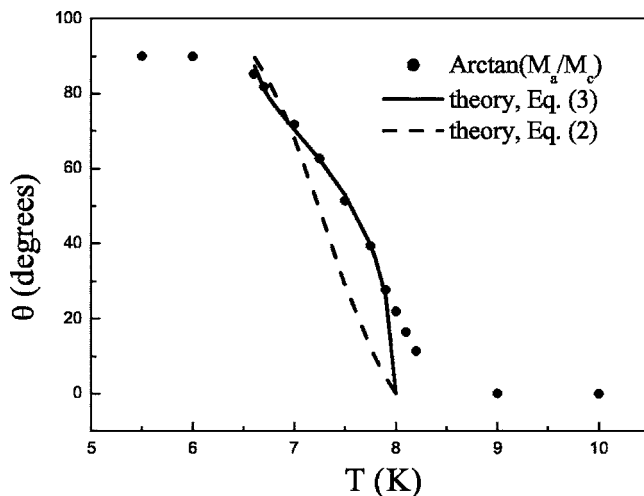


FIG. 6. Magnetization rotation angle  $\theta(T)$  calculated from experimental data in the reorientation region  $[T_2, T_1]$  at zero external magnetic field. Solid curve: theory Eq. (3), dash curve: conventional theory Eq. (2)

$\ll T_N$ . The free energy of the iron subsystem is taken in the form

$$F(\theta, T) = F_0(T) + \frac{K_u(T)}{2} \cos(2\theta) + K_b \cos(4\theta). \quad (1)$$

With minimal assumptions about the temperature dependence of phenomenological constants inside the reorientation region, namely, constant  $K_b$  and  $K_u(T)$  linearly varying with temperature and going through zero inside the reorientation interval, the minimization of the conventional energy functional (1) gives<sup>2,7,8</sup>

$$\tan \theta = \sqrt{\frac{1 + \xi}{1 - \xi}}, \quad \xi(T) = \frac{(T_1 + T_2)/2 - T}{(T_1 - T_2)/2}. \quad (2)$$

Figures 5 and 6 show that experimental results neither support the constancy of  $M(T)$ , nor give a  $\theta(T)$  dependence consistent with Eq. (2)

According to the modified mean field model, paramagnetic susceptibility of ytterbium subsystem should also be taken into account to adequately describe the magnetic behavior of the orthoferrite. It is assumed, that in the molecular field of iron the rare-earth ion acquires a magnetic moment  $\mathbf{m} = \hat{\chi}^{\text{Yb}} \mathbf{F}$ , while the absolute value of the iron moment  $\mathbf{F}$  remains constant.<sup>1,8,13,14</sup> Experimentally measured magnetization is the sum of the iron and rare-earth contributions  $\mathbf{M} = \mathbf{F} + \mathbf{m}$ . The magnetic susceptibility  $\hat{\chi}^{\text{Yb}}$  of the rare-earth ions is assumed to be anisotropic. This assumption naturally explains the large change of  $M$  inside a narrow temperature interval, since rotation of  $\mathbf{F}$  leads to the change of  $\mathbf{m}$  and thus changes  $M$  as well.<sup>9</sup> The anisotropy of the rare-earth susceptibility has been reported in the literature.<sup>1,8,13,14</sup> The key point of Ref. 9 was the proper account of such anisotropy in the calculation of the rotation angle and absolute value of the magnetization, with the result

$$\tan \theta = r \sqrt{\frac{1 + \xi}{1 - \xi}}, \quad r = \frac{M_a(T_2)}{M_c(T_1)}, \quad (3)$$

$$M = M_c(T_1) \sqrt{\frac{r^2(1 + \xi) + (1 - \xi)}{2}}. \quad (4)$$

Since  $M_a(T_2)$  and  $M_c(T_1)$  are measurable magnetizations of the sample at temperatures  $T_2$  and  $T_1$ , respectively, the value of  $r$  is known and expressions (3) and (4) have no fitting parameters.

According to our measurements, the cubic sample A had  $T_1=8.0$  K and  $T_2=6.6$  K. Using the values of  $M_a(T_2)$  and  $M_c(T_1)$  at these temperatures we find  $r=1.78$  for this sample. Theoretical curves given by Eqs. (3) and (4) are shown in Figs. 5 and 6 by solid lines. A convincing correspondence between the theory and experiment is evident.

Note, that the analysis of experimental data in terms of the model introduced in Refs. 9,10 is only valid inside the reorientation region. However, it is important that inside the region of its validity such analysis is independent of the driving mechanism of the transition, be it the interactions in the iron subsystem, the  $R$ -Fe interactions, the behavior of the rare-earth magnetic susceptibility, or any other process. The approach of Refs. 9,10 only requires the effective anisotropy constant  $K_u(T)$  to be a linear function of temperature. Since precisely that behavior of  $K_u(T)$  was measured in Refs.

15,16, and Ref. 17 shows that such behavior follows from the microscopic model of Ref. 18, the modified mean field theory<sup>9,10</sup> can be applicable for a wide variety of orthoferites.

#### IV. CONCLUSION

In this paper we report direct measurements of the magnetization absolute value  $M(T)$  and rotation angle  $\theta(T)$  during the  $\Gamma_4 \rightarrow \Gamma_{24} \rightarrow \Gamma_2$  spin-reorientation transition in  $\text{YbFeO}_3$  single crystals. The results favor the importance of strongly anisotropic rare-earth contribution to the magnetization of the material. They give a convincing argument in favor of the spin reorientation model suggested in Ref. 9 and its applicability to  $\Gamma_4(G_x, F_z) \rightarrow \Gamma_{24}(G_{xz}, F_{xz}) \rightarrow \Gamma_2(G_z, F_x)$  orientation transitions in different materials.

#### ACKNOWLEDGMENTS

The work at O. Galkin Physics & Technology Institute was partially supported by the State Fund for Fundamental Research of Ukraine, Project No. F7/203-2004. Ya.B. was supported by DARPA/ARO, Contract No. DAAD19-01-C-006.

<sup>1</sup>R. White, J. Appl. Phys. **40**, 1061 (1969).

<sup>2</sup>K. P. Belov, A. K. Zvezdin, A. M. Kadomtseva, and R. V. Levitin, *Orientation Phase Transitions in Rare Earth Magnetic Materials* (Nauka, Moscow, 1979) (in Russian).

<sup>3</sup>V. D. Buchel'nikov, N. K. Dan'shin, L. T. Tsymbal, and V. G. Shavrov, Phys. Usp. **39**, 547 (1996).

<sup>4</sup>V. D. Buchel'nikov, N. K. Dan'shin, L. T. Tsymbal, and V. G. Shavrov, Phys. Usp. **42**, 957 (1999).

<sup>5</sup>A. V. Kimel, A. Kirilyuk, A. Tsvetkov, R. V. Pisarev, and Th. Rasing, Nature (London) **429**, 850 (2004).

<sup>6</sup>A. V. Kimel, A. Kirilyuk, P. A. Usachev, R. V. Pisarev, A. M. Balbashov, and Th. Rasing, Nature (London) **435**, 655 (2005).

<sup>7</sup>J. R. Shane, Phys. Rev. Lett. **20**, 728 (1968); H. Horner and C. M. Varma, *ibid.* **20**, 845 (1968).

<sup>8</sup>J. Sirvardiere, Solid State Commun. **7**, 1555 (1969).

<sup>9</sup>Ya. B. Bazaliy, L. T. Tsymbal, G. N. Kakazei, A. I. Izotov, and P. E. Wigen, Phys. Rev. B **69**, 104429 (2004).

<sup>10</sup>Ya. B. Bazaliy, L. T. Tsymbal, G. N. Kakazei, and P. E. Wigen, J. Appl. Phys. **95**, 6622 (2004).

<sup>11</sup>V. G. Baryakhtar, A. N. Bogdanov, and D. A. Yablonskii, Sov. Phys. Solid State **29**, 65 (1987).

<sup>12</sup>R. M. Bozorth, V. Kramer, and J. P. Remeika, Phys. Rev. Lett. **1**, 3 (1958).

<sup>13</sup>D. Treves, J. Appl. Phys. **36**, 1033 (1965).

<sup>14</sup>T. Yamaguchi, J. Phys. Chem. Solids **35**, 479 (1974).

<sup>15</sup>M. Abe, M. Gomi, K. Shono, Y. Mori, and S. Nomura, Jpn. J. Appl. Phys. **16**, 279 (1977).

<sup>16</sup>K. P. Belov, R. A. Volkov, B. P. Goranskii, A. M. Kadomtseva, and V. V. Uskov, Fiz. Tverd. Tela (Leningrad) **11**, 1148 (1969) [Sov. Phys. Solid State **11**, 935 (1969)].

<sup>17</sup>W. J. Schaffer, R. W. Bene, and R. M. Walser, Phys. Rev. B **10**, 255 (1974).

<sup>18</sup>L. M. Levinson, M. Luban, and S. Shtrikman, Phys. Rev. **187**, 715 (1969).